1992-12

A calibration of the Naval Postgraduate School Middle Ultraviolet Spectrograph (MUSTANG).

Chase, Bruce E.

Monterey, California. Naval Postgraduate School

NAVAL POSTGRADUATE SCHOOL
Monterey, California

THESIS

A Calibration of the Naval Postgraduate School
Middle Ultraviolet Spectrograph (MUSTANG)

by

Bruce E. Chase

December 1992

Thesis Advisor: David D. Cleary

REPORT DOCUMENTATION PAGE

Form Approved
OMB No. 0704-0188

1a REPORT SECURITY CLASSIFICATION: Unclassified	1b RESTRICTIVE MARKINGS
2a SECURITY CLASSIFICATION AUTHORITY	3 DISTRIBUTION / AVAILABILITY OF REPORT: Approved for public release;distribution is unlimited.
2b DECLASSIFICATION / DOWNGRADING SCHEDULE	
4 PERFORMING ORGANIZATION REPORT NUMBER(S)	5 MONITORING ORGANIZATION REPORT NUMBER(S)
6a NAME OF PERFORMING ORGANIZATION: Naval Postgraduate School; 6b OFFICE SYMBOL (If applicable): 33	7a NAME OF MONITORING ORGANIZATION: Naval Postgraduate School
6c ADDRESS (City, State, and ZIP Code): Monterey, CA 93943-5000	7b ADDRESS (City, State, and ZIP Code): Monterey, CA 93943-5000
8a NAME OF FUNDING / SPONSORING ORGANIZATION; 8b OFFICE SYMBOL (If applicable)	9 PROCUREMENT INSTRUMENT IDENTIFICATION NUMBER
8c ADDRESS (City, State, and ZIP Code)	10 SOURCE OF FUNDING NUMBERS: PROGRAM ELEMENT NO; PROJECT NO; TASK NO; WORK UNIT ACCESSION NO

11 TITLE (Include Security Classification): A Calibration of the Naval Postgraduate School's Middle Ultraviolet Spectrograph (MUSTANG)

12 PERSONAL AUTHOR(S): Chase, Bruce, E.

13a TYPE OF REPORT	13b TIME COVERED	14 DATE OF REPORT (Year, Month, Day)	15 PAGE COUNT
Master's Thesis	FROM _____ TO _____	December 1992	60

16 SUPPLEMENTARY NOTATION: The views expressed in this thesis are those of the author and do not reflect the official policy or positions of the Department of Defense or the U.S. Government.

17 COSATI CODES			18 SUBJECT TERMS (Continue on reverse if necessary and identify by block number)
FIELD	GROUP	SUB-GROUP	Spectrograph; Ultraviolet spectra; Airglow

19 ABSTRACT (Continue on reverse if necessary and identify by block number)

The Naval Postgraduate School's Middle Ultraviolet Spectrograph (MUSTANG) was designed to measure the spectrum of the Earth's airglow from 1800 A to 3400 A. The MUSTANG instrument was tested using standard techniques to determine the wavelength calibration overall sensitivity, and detector linearity. The instrument was launched on a NASA sounding rocket on March 19, 1992, from White Sands Missile Range N.M. Post-flight tests indicate that the calibration did not change as a result of the rocket experiment.

20 DISTRIBUTION / AVAILABILITY OF ABSTRACT: ☒ UNCLASSIFIED/UNLIMITED ☐ SAME AS RPT ☐ DTIC USERS	21 ABSTRACT SECURITY CLASSIFICATION
22a NAME OF RESPONSIBLE INDIVIDUAL: David D. Cleary	22b TELEPHONE (Include Area Code): (408) 646-2828; 22c OFFICE SYMBOL: PH/Cl

DD Form 1473, JUN 86 — Previous editions are obsolete — S/N 0102-LF-014-6603

Approved for public release; distribution is unlimited.

A Calibration of the Naval Postgraduate School Middle Ultraviolet Spectrograph (MUSTANG)

by

Bruce E. Chase
Lieutenant, United States Navy
B.S., University of Mississippi

Submitted in partial fulfillment
of the requirements for the degree of

MASTER OF SCIENCE IN PHYSICS

from the

NAVAL POSTGRADUATE SCHOOL
December 1992

Author: [redacted]
Bruce E. Chase

Approved by: [redacted]
David D. Cleary, Thesis Advisor

[redacted]
Suntharalingam Gnanalingam, Co-Thesis Advisor

[redacted]
Karlheinz E. Woehler, Chairman, Department of Physics

ABSTRACT

The Naval Postgraduate School's Middle Ultraviolet Spectrograph (MUSTANG) was designed to measure the spectrum of the Earth's airglow from 1800 Å to 3400 Å. The MUSTANG instrument was tested using standard techniques to determine the wavelength calibration, overall sensitivity, and detector linearity. The instrument was launched on a NASA sounding rocket on March 19, 1992, from White Sands Missile Range N.M. Post-flight tests indicate that the calibration did not change as a result of the rocket experiment.

TABLE OF CONTENTS

LIST OF TABLES

LIST OF FIGURES

ACKNOWLEDGEMENT

To my wife, Julie. Without your love and support I could not have completed my studies at Naval Postgraduate School. To my thesis advisor, Dave Cleary. Thanks for displaying the patience of Job. To my thesis co-advisor, 'Gnani' Gnanalingam. Thanks for your many hours of assistance with the theory and calibration. To my labmates, thanks for all the help. And to my pal Cal, thanks for providing that wagging tail on those rough days.

I. INTRODUCTION

This work focuses on the calibration of the Naval Postgraduate School's Middle Ultraviolet Spectrograph (MUSTANG). The MUSTANG instrument was launched on a NASA sounding rocket and was designated for remote sensing of the earth's ionosphere. The ionosphere is a region of the atmosphere where the electron densities are sufficiently high to form a plasma. Research of the earth's ionosphere has significant military applications, as the ionosphere can affect such systems as high frequency radio communications, over-the-horizon radar, ballistic missile early warning, and the ground wave emergency network.

The current method of sounding the ionosphere is from ground-based ionosonde stations. This method is effective locally, but is not accurate on a large scale. A rocket launched sounding instrument allows the instrument to effectively see through a limb of the earth. An inherent disadvantage of the rocket launched sounding instrument is that it only observes what is occurring as it passes through the atmosphere. A satellite-based sounding instrument would be an excellent method of forecasting the ionosphere. To this end the Department of Physics at NPS is building a second generation MUSTANG. This detector system has been named the Ionospheric Spectroscopy And Atmospheric Composition (ISAAC)

instrument. ISAAC is scheduled to be flown on the Air Force satellite ARGOS in 1995.

A. THESIS OBJECTIVES

The goal in this thesis was a calibration of the MUSTANG instrument. An accurate calibration is necessary to allow precise analysis of experimental data in order to provide a basis for comparison with theoretical models.

B. THESIS OUTLINE

The thesis is divided into five chapters. Chapter II provides an overview of the atmosphere, ionosphere, and airglow. Chapter III describes the experiment and the MUSTANG instrument. The ground support equipment and laboratory data collection are also explained. Chapter IV provides a detailed description of the calibration. Chapter V concludes the thesis and makes recommendations for future research.

II. BACKGROUND

A. THE NEUTRAL ATMOSPHERE

The earth's atmosphere has a number of distinct layers. These layers are most commonly characterized by either temperature or chemical composition. A temperature profile along with the corresponding layers is shown in Figure 1. The lowest temperature-designated layer is the troposphere. The troposphere extends from the earth's surface to about 15 km. This region is characterized by a negative temperature gradient. The tropopause marks the top of the troposphere and the beginning of the stratosphere. The stratosphere extends to about 50 km. Ozone (O_3) exists in this region in sufficient quantities to absorb solar radiation. This produces a positive temperature gradient. The stratopause marks the top of the stratosphere and the beginning of the mesosphere. The mesosphere extends to about 85 km. In the mesosphere the temperature gradient is negative. The mesopause marks the end of the mesosphere and the beginning of the final region of the atmosphere, the thermosphere. In the thermosphere temperature increases with altitude until an equilibrium temperature is reached. This equilibrium temperature depends on solar radiation and usually varies between 1000K and 1800K.

Another method used for classification of the atmosphere is by chemical composition. This method leads to three horizontal regions. The first region is referred to as the homosphere. In this region the mean molecular composition remains fairly constant due to vertical mixing. The top of the homosphere is marked by the turbopause. Below the turbopause the scale heights of atmospheric constituents are the same. In the heterosphere the primary transport mechanism is diffusion. Diffusion causes the distribution of atmospheric constituents to change with altitude, resulting in individual scale heights. The heterosphere extends from the homosphere up to about 500 kilometers. The final region is referred to as the exosphere. In the exosphere the molecular densities are so low that particle trajectories are essentially parabolic orbits. The exosphere extends from 500 km until the earth's atmosphere blends with space.

B. THE IONOSPHERE

The ionosphere is defined as that portion of the upper atmosphere where ions and electrons are present in sufficient quantities to create a plasma . This plasma can affect radiowave propagation. Most of these electrons and ions are produced when electromagnetic radiation (photons) from the sun strikes neutral molecules with sufficient energy to liberate electrons. This process is referred to as photoionization. The reaction describing the ionization of a molecule Q is

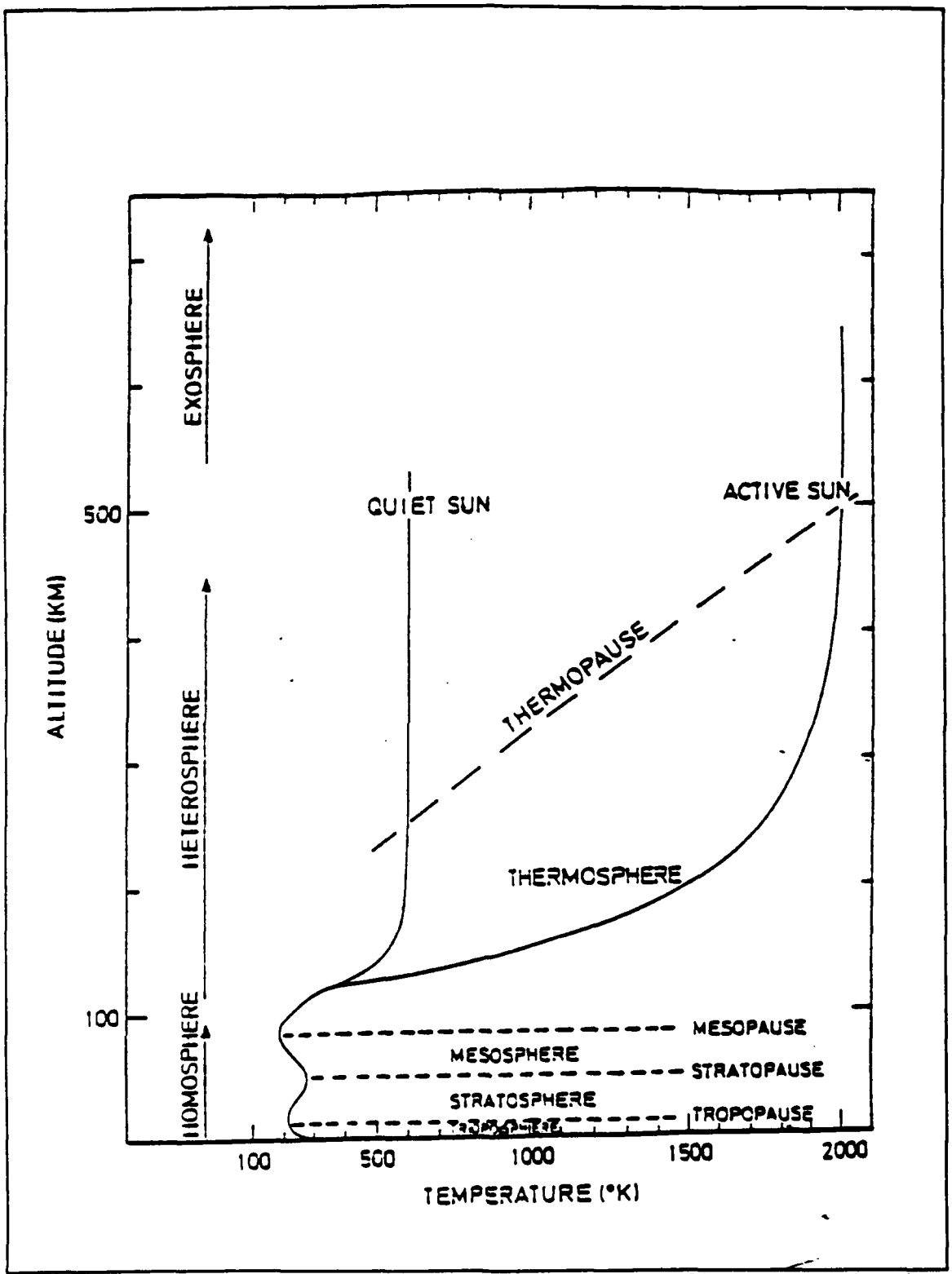

Figure 1. Temperature Profile and Corresponding Atmospheric Layers

$$Q + h\nu \rightarrow Q^{+} + e^{-} .$$

The rate of this reaction depends on three factors: The number of molecules exposed to the electromagnetic radiation, the number of photons available, and the efficiency with which these photons cause ionization. This efficiency is wavelength dependent and is referred to as the ionization cross-section.

The concentration of molecules decreases with increasing altitude and the photon flux decreases with decreasing altitude. Consequently, the rate of ionization, which is proportional to the product of the molecular concentration and the photon flux, has a distinct maximum. The curve which depicts the variation of the ionization rate with altitude is referred to as a Chapman ionization profile (See Figure 2). Chapman was the first to provide a quantitative explanation for the formation of an ionized layer (Chapman, 1931).

The division of the ionosphere into layers is due to the presence of distinct electron density plateaus. These distinct layers develop because solar energy is deposited at different altitudes and the composition of the atmosphere changes with altitude. The ionosphere is categorized by these layers. They are labeled D, E, and F, the latter being further divided into F1 and F2.

The D region is the lowest layer of the ionosphere. It extends from about 50 to 90 km. Ionization is primarily due to absorption of solar Lyman-alpha radiation by nitric oxide. The chemical reaction is written

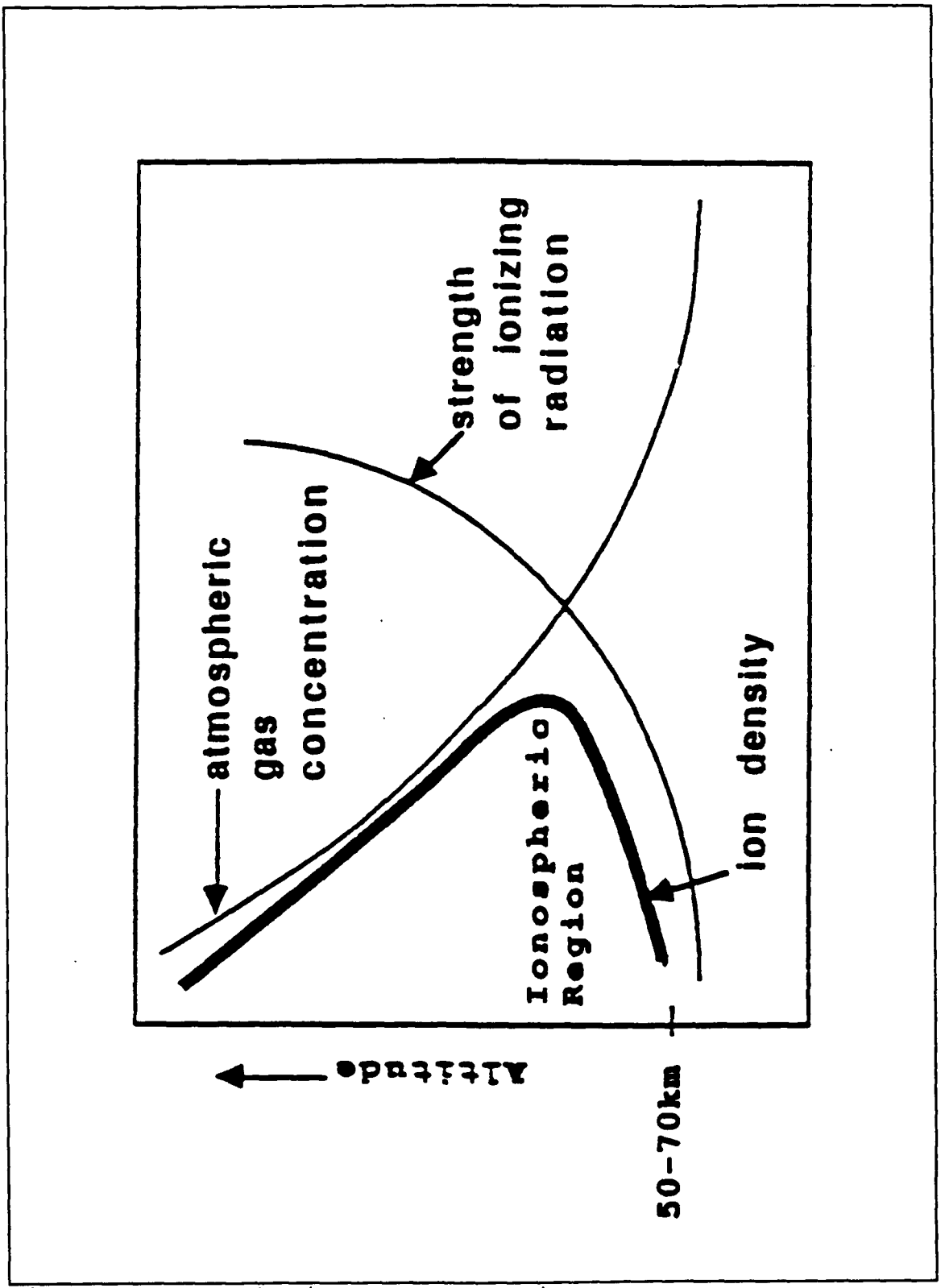

Figure 2. Ionospheric Layer Formation

$$NO + h\nu \rightarrow NO^{+} + e^{-} .$$

This region is a weakly ionized plasma. The electron densities range from 10^2 to 10^4 (el cm^{-3}) during the day, to almost zero at night. The primary charge carriers in this region are O_2^{+}, NO^{+}, and NO_2^{-}. The most prevalent reactions at night are

$$NO^{+} + e^{-} \rightarrow N + O$$

and

$$O_2^{+} + e^{-} \rightarrow O + O .$$

These reactions are called dissociative recombination, and they explain why the D layer disappears at night.

The E region extends from 90 to 140 km. The primary method of ion production is the ionization of molecular oxygen from solar extreme ultraviolet and soft x-rays. The major charge carriers in this region are, NO^{+}, O_2^{+}, and O^{+}. This region is a stronger plasma than the D region. The electron densities range from about 1.5 X 10^5 (el cm^{-3}) during the day, to a night density of around 1 x 10^4 (el cm^{-3}). The E-region exists at night because its recombination rate is slower.

The region of greatest interest to the military is the F region. The plasma in the F region is sufficiently dense to cause reflection of high-frequency radio communication waves and is used for over-the-horizon targeting. The F region is divided into two layers called F1 and F2. The F1 region extends from 140 to 200 km, and the daytime electron density peaks at 2.5 x 10^5 (el cm^{-3}). The principal ion formed in this region is O^{+} , with some contribution by O_2^{+} and NO^{+}. They are

formed by solar flux from Lyman and Helium emission lines. These emissions disappear at night and the ions produced have a short lifetime. This causes the F1 region to disappear at night.

The F2 region extends from 160 to 600 km. The ion production process is the same as the F1 layer. However, in the F2 region other factors affect the ionization profile. At high altitudes ion-atom interchange is the dominant loss mechanism. Because this rate decreases more rapidly with altitude than the ionization production rate, in photochemical equilibrium one would expect the O^+ density to increase indefinitely with altitude. This is not the case though. The F2 region reaches a point where the chemical lifetime is longer than the diffusion lifetime. Ambipolar diffusion causes positive ions to diffuse downwards out of the region.

C. AIRGLOW

The objective of the MUSTANG experiment was to investigate solar energy deposition and the associated photochemical mechanisms in the ionosphere. This was accomplished by observing emission's in the earth's airglow. Density profiles can be inferred from airglow emissions. The density profiles of neutral atoms and molecules can be used to infer electron and ion densities.

Airglow is the naturally-occurring emission of radiation by the earth's atmosphere. It includes the energy spectrum

from the far ultraviolet to the near infrared. We can differentiate between airglow and aurora because auroras are sporadic in nature and exist in magnetic polar and subpolar regions. The three greatest contributors of airglow are direct sunlight scattering, electron impact excitation and photochemistry of neutral constituents.

Direct sunlight scattering, also referred to as photoexcitation, is the primary source of airglow during the day. Photoexcitation occurs when a photon undergoes an inelastic collision with an atom or molecule. The photon is absorbed by the atom and is excited to a higher energy state. A transition to a lower energy state results in the emission of a photon of energy equal to the difference in energy states.

Multiple photons can be emitted when there are intermediate states between the excited state and ground state. Atoms have only electronic states. Molecules have electronic, vibrational, and rotational states. Molecular transitions can occur between any two combinations of these. Transitions are classified as either allowed or forbidden by virtue of their compliance with certain quantum selection rules. A transition that satisfies all selection rule requirements is an allowed transition. A transition that violates a selection rule is referred to as forbidden.

Electron impact excitation can cause a particle to make a transition to an excited state where it can emit a photon by

undergoing a forbidden transition. Another source of airglow emission is from the photochemistry of neutral particles. The photochemical processes consists of the absorption of a photon by a molecule. This puts the molecule in an excited rotational or vibrational level or an excited electronic state. From this excited state the molecule can enter secondary chemical reactions. After the chemical interaction the new species emits a photon. This process is called chemiluminescence. Although chemiluminescence is relatively insignificant during the day, it can be significant at night when other excitation sources are not present.

III. EXPERIMENT

A. INTRODUCTION

The purpose of the experiment was to investigate the solar energy deposited and the photochemical reactions taking place in the ionosphere. This was accomplished by detecting the earth's natural ultraviolet emissions. According to theoretical calculations ionospheric electron density can be inferred by measuring airglow. This was tested by conducing a NASA rocket experiment. The rocket payload consisted of the Naval Research Laboratory's (NRL) High Resolution Airglow and Aurora Spectrograph (HIRAAS) and the Naval Postgraduate School's (NPS) MUSTANG. Together these instruments covered a wavelength range 500Å - 3400Å. The instruments were launched on board a NASA Terrier Black Brant sounding rocket on March 19, 1992. The sounding rocket is depicted in Figure 3. The door on the payload section opened at approximately 100 km. When the payload had completed outgassing the attitude control system maneuvered the payload so the instrument zenith-look-angle was 100 degrees. Data were then taken on the upleg from 150 km to the apogee altitude of 320 km. Data were taken on the downleg from 320 km to 115 km with the zenith look angle at 90 degrees. The data received from the MUSTANG instrument were transferred via rocket telemetry to a ground station. The

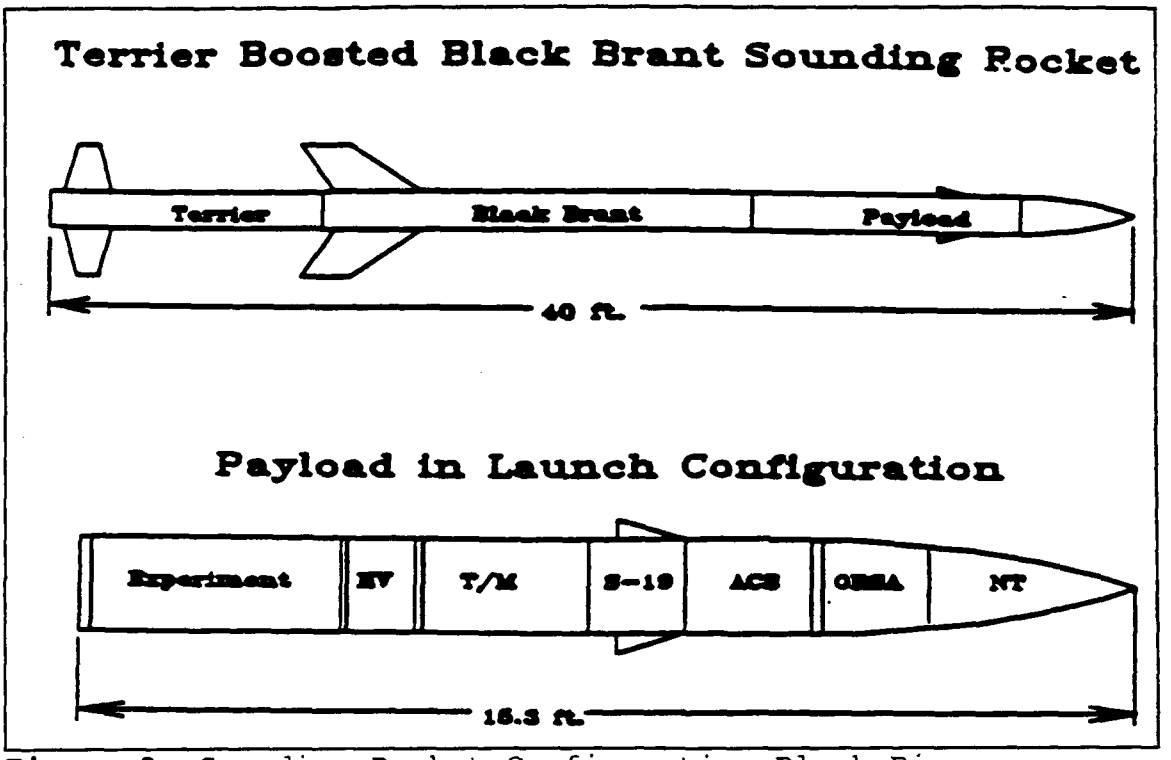

Figure 3. Sounding Rocket Configuration Block Diagram

payload section of the rocket landed 50 miles uprange after a parachute-retarded final descent.

B. INSTRUMENT DESCRIPTION

The MUSTANG instrument is a 1/8th meter Ebert-Fastie spectrograph with a 1/8th meter telescope. The instrument was fabricated by Research Support Instruments, Inc. The wavelength coverage is from 1800Å to 3400Å which is the middle ultraviolet portion of the electromagnetic spectrum. A photodetector consisting of an image intensifier optically coupled to a linear photodiode array is positioned at the exit focal plane of the spectrograph. The voltage output from each of the 512 photodiodes is proportional to the

corresponding light intensity. The electronics interface was constructed at the Naval Postgraduate School. A schematic diagram of the MUSTANG instrument is depicted in Figure 4. A more detailed explanation of the MUSTANG instrument is given in the sections to follow.

1. Ebert-Fastie Spectrograph

The ultraviolet light which enters the telescope is collected by a 1/8th meter spherical mirror. This mirror focuses light onto a 5mm by 140um vertical slit. After passing through the entrance slit the light strikes the Ebert mirror. This mirror colimates the light and directs it onto a

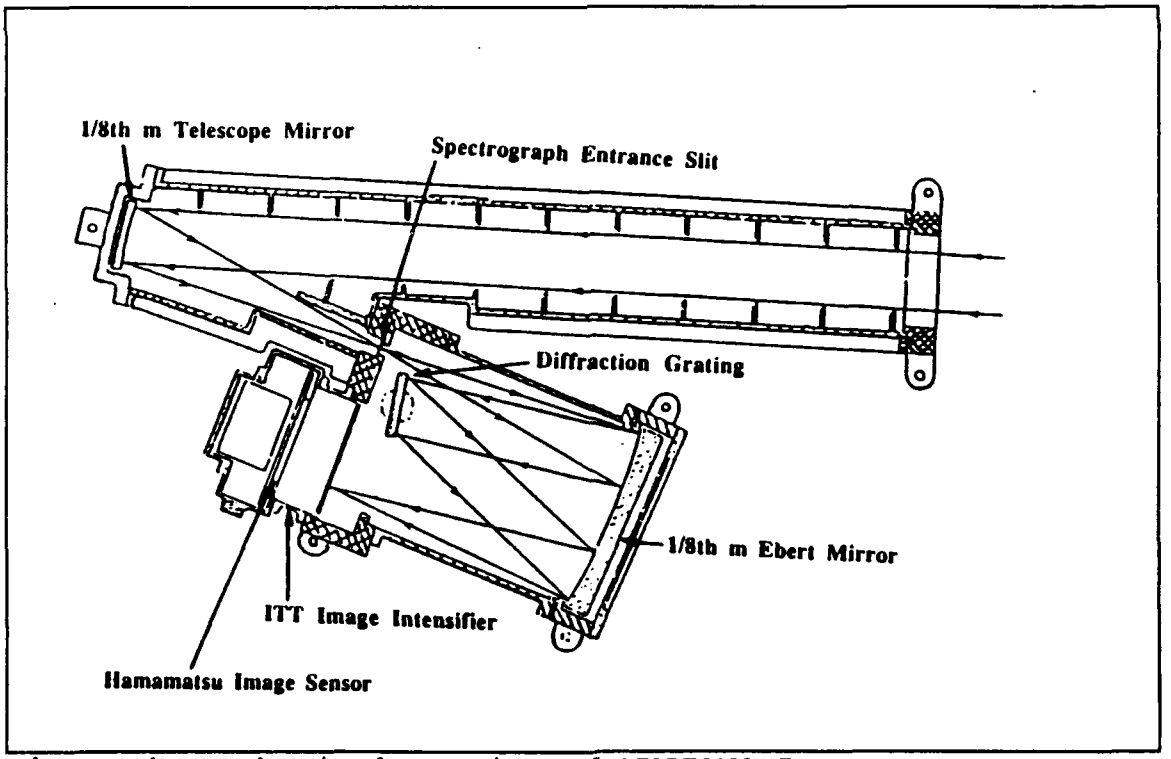

Figure 4. Mechanical Drawing of MUSTANG Instrument

reflective diffraction grating. The grating was produced by HYPERFINE and has a line spacing of 1200 lines/mm. The grating reflects the colimated light back to the Ebert mirror where it is then focused onto the image intensifier at the spectrograph focal plane.

2. ITT Image Intensifier

The light striking the image intensifier has a bandwidth of 1800Å to 3400Å. The image intensifier is an ITT F4145 proximity focused channel intensifier tube with dual microchannel plates. It consists of a quartz input window, a cesium telluride (CsTe) photo-cathode, two microchannel plates (MCP) in cascade, an aluminum screen coated with phosphor, and a fiber optic output window. The purpose of the image intensifier is to produce a gain so the incoming ultraviolet (UV) photons can be converted to visible photons and then be detected by the image sensor. Ultraviolet photons at the exit focal plane of the spectrograph strike the photo-cathode causing photo-electrons to be generated. These electrons are accelerated toward the microchannel plates by an accelerating voltage of approximately 2000 Volts. As the photo-electrons strike the walls of the MCP an electron avalanche occurs. The result is that approximately 40,000 electrons are produced for every one emitted by the photo-cathode. These electrons are again accelerated by 6,000 Volts between the MCP and the phosphor screen. The screen fluoresces as a result of the

bombarding electrons. This visible light is transmitted through a fiber optic window with the same spatial configuration as the original spectrum incident on the photo-cathode.

3. Hamamatsu Linear Image Sensor

The Hamamatsu S2300-512F Plasma-Coupled Device (PCD) Linear Image Sensor is a monolithic self-scanning photodiode array. The photodiodes are sensitive to light in the 4000Å to 10000Å region. Photons emitted from the image intensifier phosphor screen are sensed by the PCD image sensor. The output window of the image intensifier and the PCD image sensor window are both made of fiber optic material. The two devices are placed physically in contact.

The monolithic PCD linear image sensor has two basic sections. A light sensitive section and a shift register transfer section. The light sensitive section is a 25mm by 5mm photosensitive area consisting of 512 photodiodes arranged in a linear array. The photodiodes are 36um wide, 5mm tall, with a spacing of 50um between the centers of each photodiode. The photodiodes convert the optical energy of incident photons to a charge. In the shift register section the charge accumulated in the photodiodes is transferred to the output.

C. DATA COLLECTION AND SUPPORTING EQUIPMENT

The laboratory Ground Support Equipment (GSE) must provide two functions. It must provide the same timing signals that

the rocket telemetry delivers the instrument during flight. The GSE must also collect the data from the MUSTANG instrument. A method to display the acquired data is necessary to ensure the MUSTANG is operating properly. The functions of the GSE described above are performed by the Macintosh II computer and National Instruments (NI) data acquisition boards. An interface box is necessary for synchronizing all of the clock signals and for providing a means to physically connect the NI data acquisition boards to the MUSTANG.

The software used with the Macintosh to take spectra is called LabVIEW and was developed by National Instruments. It is an object oriented programming language and individual programs are depicted on the screen in the form of icons. To take calibration data only a few steps are required. These steps are accomplished by clicking on the appropriate icons. The steps necessary for taking a spectrum are outlined below:

1) Ensure all cables are connected from Macintosh to GSE box, from GSE box to MUSTANG, and from power supply to GSE box.

2) Turn on Macintosh and find the file Main GSE. Double click on this icon to launch Labview and the MUSTANG program.

3) Click on the Initialize I/O Boards icon. This initializes the data acquisition boards in the Macintosh computer.

4) Click on the Initialize Telemetry Clocks icon. This ensures that the data acquisition boards provide the correct telemetry signals to the MUSTANG instrument.

5) Turn on amp switch and high voltage switch on the GSE box. The amp switch turns on the linear array detector and the high voltage switch turns on the image intensifier tube. This energizes the MUSTANG instrument.

6) Click on the Data Acquisition icon. This launches the data acquisition program. It is important that step five be executed prior to step six. If the MUSTANG instrument is not powered it will not return a signal. The data acquisition program will wait for signals in an infinite loop.

7) Click on the Save icon. This saves the spectrum. A new spectrum can be generated by clicking on the Reacquire icon.

8) Click on the Quit icon. This stops the data acquisition subroutine and returns to the GSE panel window. Now click on Quit icon in main GSE panel window. This stops the LabView program.

9) Turn off power supply and turn off the amp and voltage switches on the GSE box.

IV. CALIBRATION

A. INTRODUCTION

The data collected from the MUSTANG instrument was recorded as a relative intensity proportional to the charge accumulated by the detector photodiodes. This charge undergoes a 10-bit analog-to-digital conversion. The result is a series of numbers that range from 0 to 1023 Decimal Units per pixel (DU/pixel). To compare the MUSTANG data with observations of airglow from other spacecraft an absolute intensity is required. When dealing with airglow we are concerned with the emission from a single atomic spectral line or a molecular spectral band. The energy emitted in the spectral features is usually of less intrinsic interest than the number of photons, which is a direct measure of the number of photochemical reactions occurring in the atmosphere. For this reason, the unit of absolute intensity used in aeronomy is the Rayleigh. The Rayleigh (R) is a measure of the omnidirectional emission rate from a column of unit cross-sectional area with $1R = 10^6$ photons/cm^2 sec. Spectropic studies use the R/Å which is an absolute intensity per unit wavelength.

Before we can convert from a relative intensity (DU/pixel) to an absolute intensity (R/Å), an instrument calibration must be conducted. The calibration will determine the detector

sensitivity. The result of the sensitivity calibration is referred to as the calibration parameter. The calibration parameter when multiplied by the detector output in Decimal Units per pixel will result in the spectral emission rate of the atmosphere. The calibration parameter is wavelength dependent and so we must first determine the precise wavelength band striking each pixel. This procedure is called a wavelength calibration. A wavelength calibration is performed not only for the sensitivity calibration but also to allow the determination of precise wavelength bands of critical emissions. In the sections to follow the calibration steps required to obtain these parameters are described. The words 'warning' and 'caution' will be used throughout the calibration process. A warning is used to alert the reader to the possibility of damage to the equipment or harm to the operator. Caution is used to bring attention to procedures that if not precisely followed could affect the outcome of the calibration.

B. CALIBRATION PROCESS

1. Wavelength Calibration

The MUSTANG instrument was designed to cover the wavelength range from 1800 Å to 3400 Å. This range was chosen because wavelengths shorter than 1800 Å are absorbed by the quartz input window of the image intensifier, and the quantum efficiency of the CsTe photo-cathode drops rapidly for

emissions of wavelengths greater than 3400 Å. The actual limits of the wavelength range striking the photodetector are controlled by varying the angle of the diffraction grating relative to the Ebert mirror. During the first NPS/NRL launch an important N_2 Second Positive band was imaged on an area of the detector where there was a defect. This drastically reduced the signal-to-noise ratio at that wavelength. As a result the N_2 second positive emission was not accurately measured. To correct this problem, for the March 1992 launch the grating was carefully rotated about a small angle. This resulted in a wavelength shift of approximately 50 angstroms. Therefore the wavelength calibration was required not only to determine the wavelength band striking each photodiode, but to ensure the grating was shifted sufficiently to allow the N_2 Second Positive emission to be measured.

A platinum lamp was used for the wavelength calibration. This platinum lamp was chosen because it had a large number of spectral emissions in the bandwidth of the instrument. The platinum lamp, in conjunction with a Hewlett Packard Harrison 6522A DC power supply, provided twenty-three known emissions in the bandwidth of coverage. Table I lists these emissions and their wavelengths.

The wavelength calibration was performed using the following procedure. The platinum lamp was placed on the optical table. The voltage setting on the Hewlett Packard Harrison 6522 A DC Power Supply was set at 400 Volts with the

Table I. SELECTED EMISSIONS OF PLATINUM HOLLOW CATHODE LAMP

Data Point	Pixel Position	Selected Emissions (Å)	
1	22.6	Ne II	1916.08
2	90.0	Pt II	2128.61
3	94.9	Pt I/II	2144.23
4	104.5	Pt I	2174.67
5	112.8	Pt I	2202.22
6	126.8	Pt II	2245.52
7	141.2	Pt I	2289.27
8	161.8	Pt I	2357.10
9	187.8	Pt I	2440.06
10	196.8	Pt I	2467.44
11	203.1	Pt I	2487.17
12	212.0	Pt I	2515.58
13	219.6	Pt I	2539.20
14	248.2	Pt I	2628.03
15	272.0	Pt I	2702.40
16	281.8	Pt I	2733.96
17	312.7	Pt I	2830.30
18	327.8	Pt I	2877.52
19	334.0	Pt I	2893.86
20	345.2	Pt I	2929.79
21	367.8	Pt I	2997.97
22	382.0	Pt I	3042.64
23	388.8	Pt I	3064.71

current limit set at 0 mA according to the manufacturers instruction.

The power supply was then energized and the current slowly increased to 15 mA. (Warning: Ensure current does not exceed 20mA or damage could occur to the platinum lamp.) Five spectra were taken and saved using Labview. For wavelength calibration the absolute intensity is not important. Therefore, the distance of the lamp to the screen and the instrument viewing angle did not matter.

It is important, however, to ensure that the instrument is not saturated. The average of five spectra obtained during preflight calibration are shown in Figure 5. The 23 emissions

of interest are identified by the numbered arrows in this figure.

The pixel positions on which the twenty-three selected emissions fell were determined by isolating each emission of interest and estimating the centroid of the emission profile. The result of this procedure is shown in Table I. A graph of wavelength verses pixel number is shown in Figure 6. The IDL function Poly_fit was used to determine the intercept and slope. The result yielded the following equation:

$$\lambda = [1848.47 + 3.134N]\,\text{Å} \qquad (4\text{-}1)$$

where N is the pixel number. Figure 6 also shows the resulting line fit. The estimated uncertainty for this fit is ±5 Å.We were concerned that when the grating was rotated it may not have been tightened sufficiently. The vibrations during launch could cause the grating to rotate further. To simulate the vibrations the detector could receive during launch it was dropped twice on its supporting platform on the optical table. A spectrum was recorded each time. First it was dropped from a height of two inches. This did not produce any noticeable change in the wavelength calibration. Next the detector was dropped from a height of three inches. This resulted in a fraction of a pixel shift. We concluded the grating was sufficiently tightened and could sustain the launch vibrations.

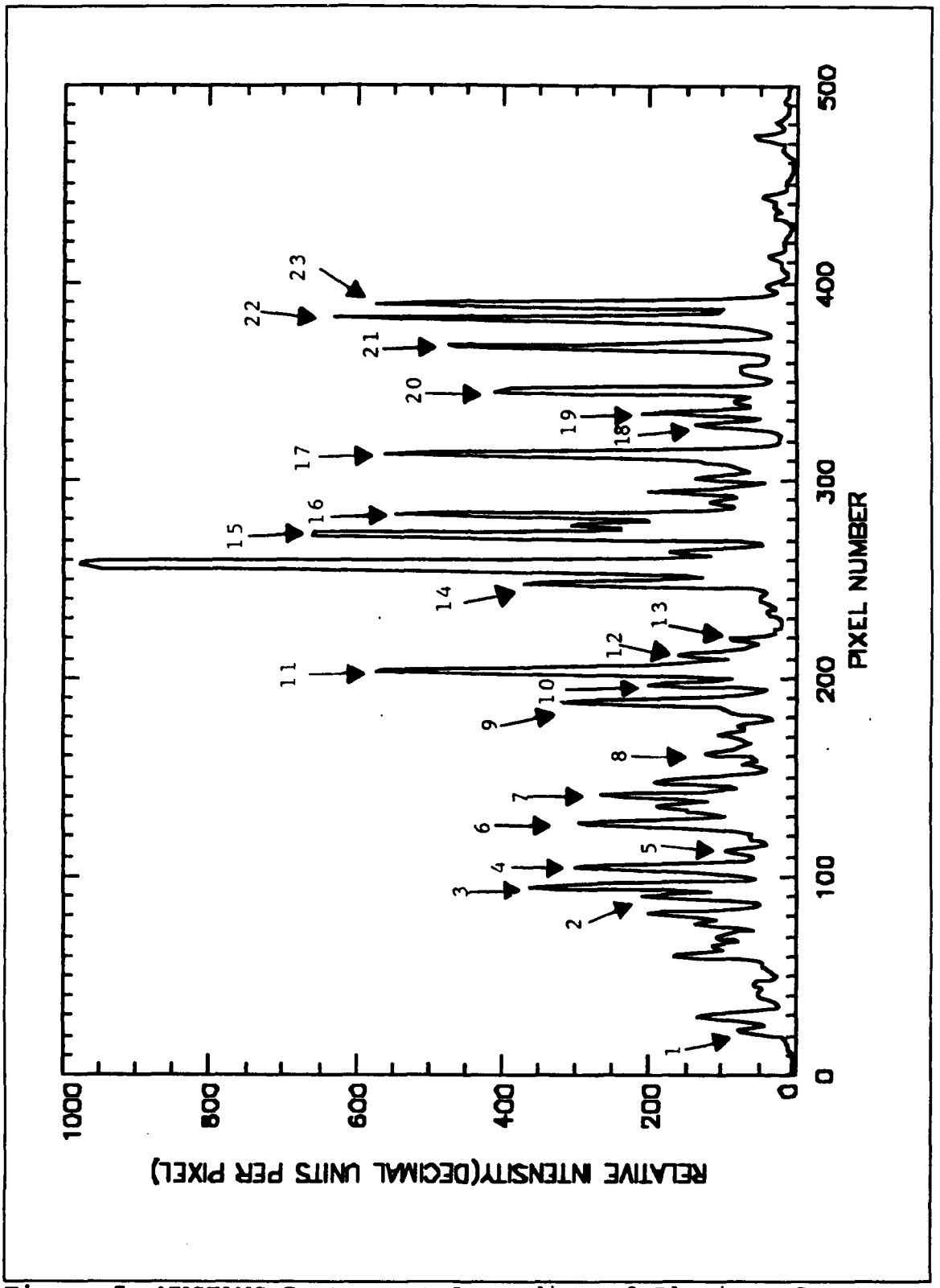

Figure 5. MUSTANG Instrument Recording of Platinum Spectrum.

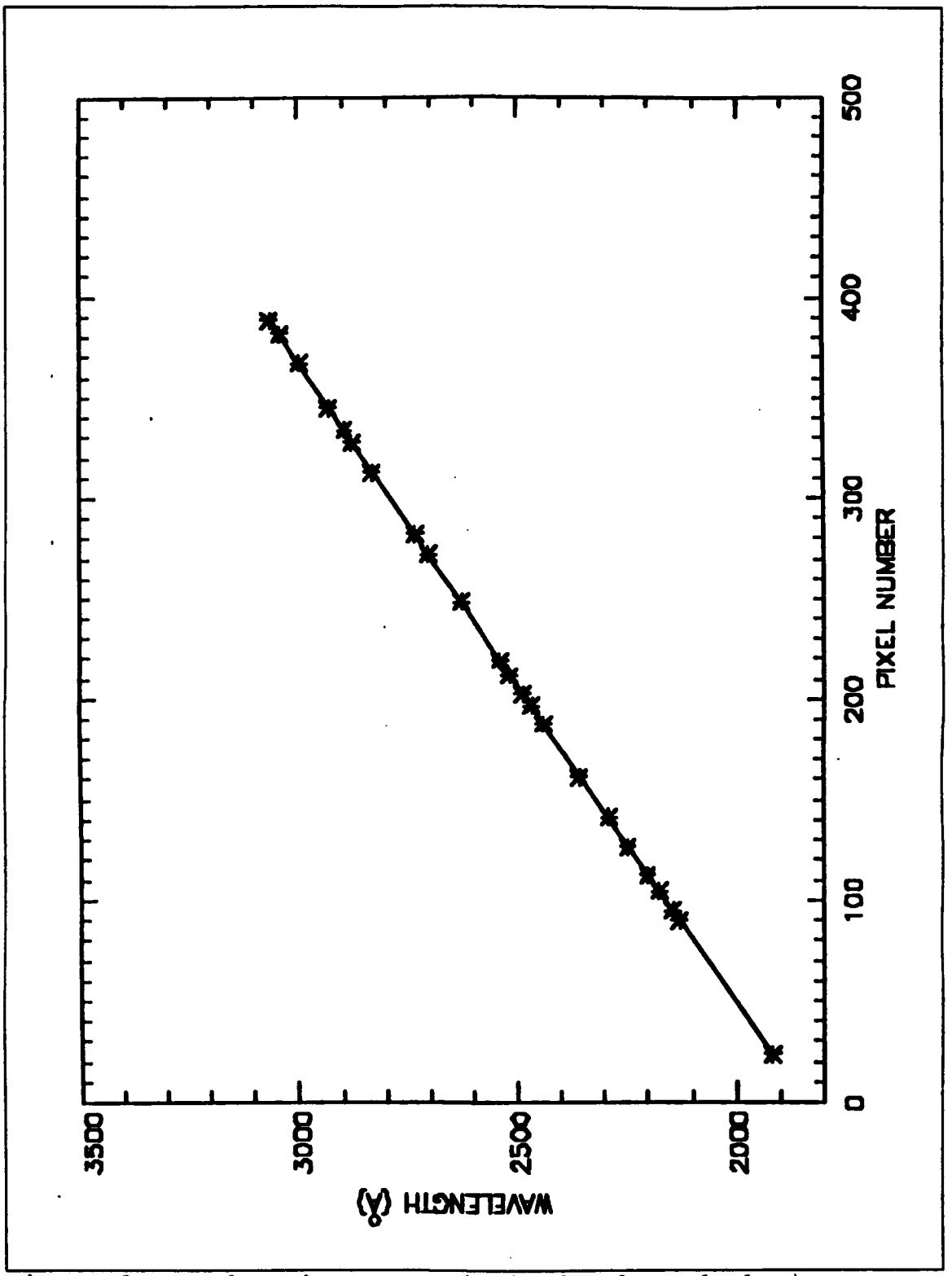

Figure 6. Wavelength Versus Pixel of Selected Platinum Emissions.

2. Sensitivity Calibration

a. *Overview*

In order to convert the output of the instrument in units of relative intensity to an absolute intensity the raw data must be multiplied by a conversion factor. This conversion factor is actually a calibration curve because it is a function of wavelength. The process of obtaining this curve is referred to as a sensitivity calibration. The sensitivity curve is obtained by measuring the detector's output response to a known input. This was accomplished by illuminating a diffusing screen with different calibrated light sources and measuring the instrument response. Two lamps were required to ensure optimal coverage of the entire wavelength band. A deuterium lamp was used for the wavelength band from 1800 Å to 2700 Å, and an FEL lamp was used for the wavelength band from 2700 Å to 3400 Å. Both lamps are traceable to the National Institute of Science and Technology (NIST).

b. *Description of Calibration*

(1) Deuterium Lamp. A deuterium lamp was used for wavelengths between 1800 Å to 2700 Å. This lamp was obtained from EG&G Gamma Scientific and had been calibrated for wavelengths from 2000 Å to 5000 Å. The deuterium lamp was powered by a Gamma Scientific 5150 power supply. This is a constant current power supply designed specifically for this

deuterium lamp. The deuterium lamp was placed 200cm from the diffusing screen.

This was chosen because the lamp did not saturate the instrument at this distance and the signal was well above the noise level. The deuterium lamp had been calibrated by the manufacturer for a distance of 50cm, so the intensity received by the screen was adjusted by $(50/200)^2$. Because of this $1/D^2$ decrease in flux precise measurement of the distance of the lamp from the screen is critical for an accurate determination of the calibration parameter. The deuterium lamp was then placed in a light-tight box with a circular iris diaphragm. (Warning: protective glasses, recommended by OSHA for UV protection, should be used around the deuterium source when it is operating.) After the deuterium source had been energized for 15 minutes the room was darkened and the iris diaphragm adjusted so the screen was fully illuminated. Ten spectra were obtained and saved with Labview.

(2) FEL Lamp. The same procedure as above was performed using a 1000-Watt FEL lamp. This is a quartz-halogen tungsten coiled-coil lamp. The FEL has a higher output than the deuterium lamp in the bandwidth 2700 Å to 3400 Å. As a result, it was placed 300cm from the screen so as to not saturate the instrument. The lamp was positioned with its identification number facing away from the measuring

instrument according to manufacturer's instruction. The lamp was connected to the Hewlett Packard 6030 power supply.

The power supply was energized and the current gradually increased to 8.00 Amperes. Setting the current at 8.00 Amps is absolutely critical as a 1% error in the current setting results in a 12% error in the spectral irradiance at 2500 Å. (Caution: In no case should one touch the quartz envelope, either hot or cold, as the resulting finger prints will burn into its surface during lamp operation.) After darkening the room, the iris diaphragm was adjusted to fully illuminate the screen. Ten spectra were taken and saved on Labview.

c. Calibration Geometry and Theory

The following definitions will be used in explaining the theory and geometry of the calibration:

E_λ- The spectral irradiance striking the screen (ph/cm^2 s Å)

L_λ- Spectral radiance leaving the screen (ph/cm^2 s Å str)

P_λ- Photon flux received over a one Å wide wavelength bin (ph/s Å)

A_t- Area (cm^2) of the telescope aperture

A_s- Area (cm^2) of the spectrograph entrance slit

A_v- Area (cm^2) of the screen viewed by the instrument

f- focal length (cm) of the telescope collecting mirror

d- distance (cm) from the telescope mirror to the screen

ρ- reflectance of the screen

The geometry of the calibration is depicted in Figure 7.

For simplicity we will represent part of this diagram with an entrance slit, a lens, and a screen. This schematic is depicted in Figure 8.

The solid angle of the slit as seen from the center of the lens is expressed as:

$$\Omega = \frac{A_s}{f^2} \qquad (4\text{-}2)$$

A ray that transverses the center of the lens will not change direction. We can therefore extend the ray from the

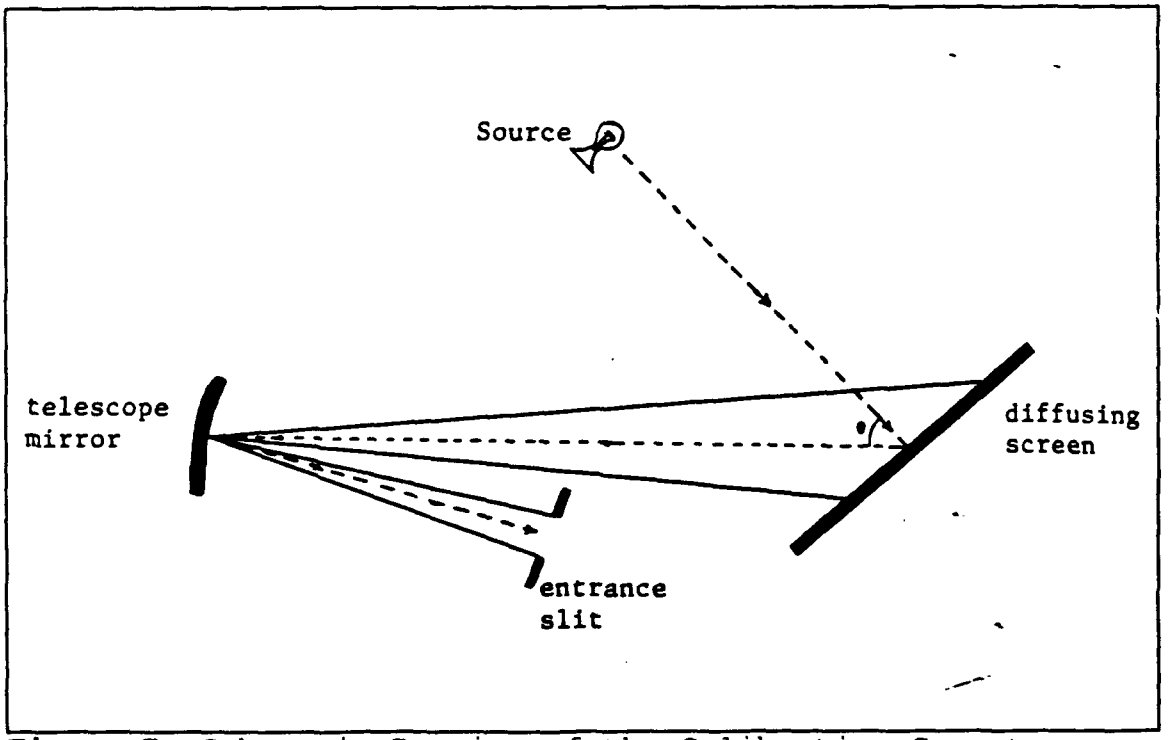

Figure 7. Schematic Drawing of the Calibration Geometry

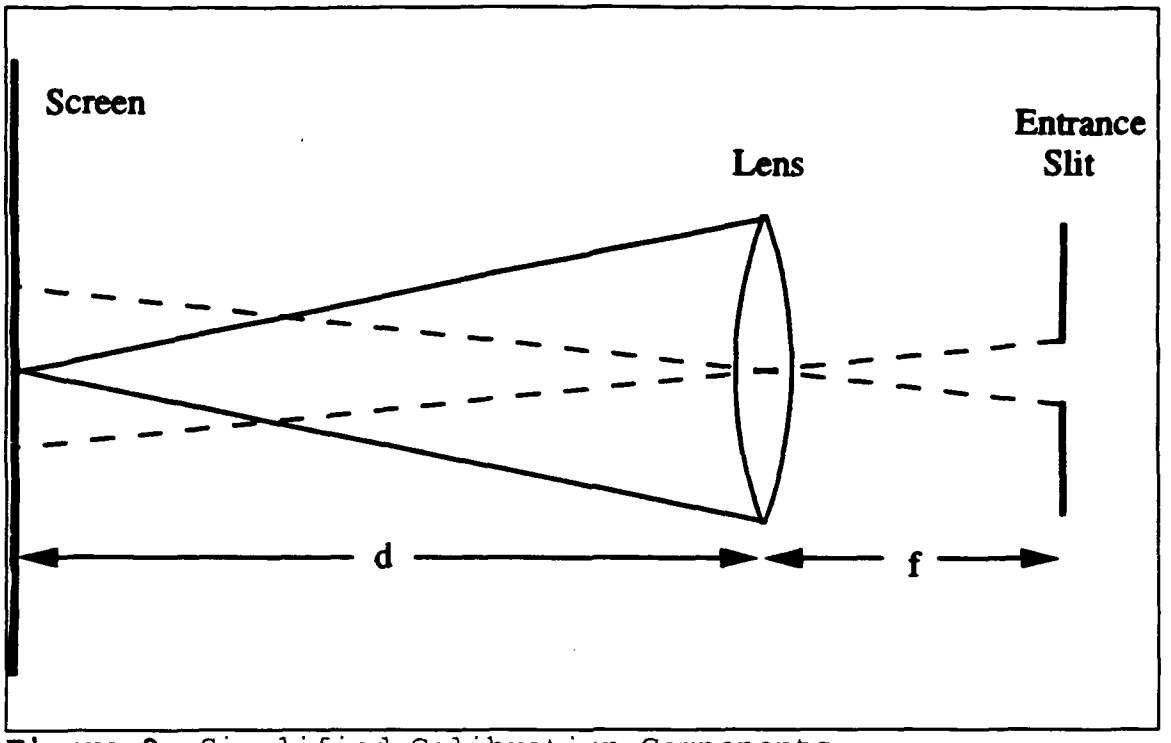

Figure 8. Simplified Calibration Components

edge of the slit through the lens and to the screen. The solid angle from the lens to the screen is the same as the solid angle from the slit to the lens and is called the instrument field-of-view. This is expressed by:

$$\Omega = \frac{A_v \cos\theta}{d^2} = \frac{A_s}{f^2} \qquad (4\text{-}3)$$

Solving for the area of the screen we obtain:

$$A_v = \frac{A_s D^2}{f^2 \cos\theta} \qquad (4\text{-}4)$$

Provided that $d^2 >> A_s$. Theta (θ) is the instrument viewing angle as depicted in Figure 7. Each small element of area on the screen emits photons in all directions. The number of photons emitted per unit area per unit time per unit solid

angle in the direction θ is $L_\lambda(\theta)$. For an ideal diffuse reflector, or Lambertian surface, the radiance at an angle θ from the normal of the screen is equal to the product of the irradiance at $\theta = 0$ times the cosine of θ, therefore $L_\lambda(\theta) = L_o\cos\theta$. The solid angle subtended by the lens at each element of area da of the screen is $\omega = (A_t/d^2)$. The number of photons per second per Angstrom received at the lens due to an element of area da is $dp = L_\lambda(\theta)\omega da$. Substituting for ω yields $dp=L(\theta)(A_t/d^2)da$.

The total number of photons received at the entrance slit of the spectrograph from the reflecting screen can be calculated by integrating over the projected area of the slit on the screen. Assuming that $L_\lambda(\theta)$ is constant over the surface of the screen the photon flux is.

$$P_\lambda = L_\lambda(\theta)\frac{A_t}{d^2}\int da. \qquad (4\text{-}5)$$

Observing that the sum of all the incremental areas is the total area of the screen viewed by the instrument we obtain:

$$P_\lambda = L_\lambda(\theta)\frac{A_t}{d^2}A_v. \qquad (4\text{-}6)$$

Substituting expression (4) for A_v yields:

$$P_\lambda = L_\lambda(\theta)\frac{A_t}{d^2}A_s\frac{d^2}{f^2\cos(\theta)}. \qquad (4\text{-}7)$$

Rearranging the terms and simplifying leaves:

$$P_\lambda = \left(\frac{A_t A_s}{f^2}\right) \frac{L_\lambda(\theta)}{\cos\theta}. \qquad (4\text{-}8)$$

Considering the screen a Lambertian surface, where $L_\lambda(\theta) = L_o \cos\theta$;

$$P_\lambda = L_o \left(\frac{A_t A_s}{f^2}\right). \qquad (4\text{-}9)$$

Therefore the number of photons per second per Angstrom passing through the entrance slit of the spectrograph is a product of constants (for constant radiance) and is independent of θ, or the distance of the screen from the lens. The above expressions show two conditions must be satisfied before a photon can make it through the entrance slit. First, it must originate in the field-of-view of the instrument. Secondly, the photon must be emitted within the solid angle defined by the area of the telescope.

The total radiance leaving the screen is equal to the irradiance striking the screen multiplied by the reflectance of the screen:

$$\int L_\lambda(\theta)\, d\Omega = E_\lambda \rho, \qquad (4\text{-}10)$$

where $d\Omega = \sin\theta d\theta d\Phi$, and the limits of integration are 0 to $\pi/2$ for θ, and 0 to 2π for Φ, because the radiance is constrained to a hemisphere. Therefore,

$$E_\lambda = \frac{\int L_\lambda(\theta)\, d\Omega}{\rho}. \qquad (4\text{-}11)$$

Since we have assumed the screen to be Lambertian the spectral irradiance is:

$$E_\lambda = \frac{1}{\rho}\int\int (L_o \cos\theta)\sin\theta d\theta d\Phi. \qquad (4\text{-}12)$$

Evaluating this integral results in $E_\lambda = \pi L_o/\rho$. Solving for the radiance normal to the screen results in:

$$L_o = \frac{\rho E_\lambda}{\pi}; \qquad (4\text{-}13)$$

and the spectral radiance is written as:

$$L_\lambda(\theta) = \frac{\rho E_\lambda}{\pi}\cos\theta. \qquad (4\text{-}14)$$

Substituting the expression for the radiance normal to the screen (4-13) into the expression for the photon flux (4-9) results in;

$$P_\lambda = \left(\frac{A_c A_s}{\pi f^2}\right)\rho E_\lambda. \qquad (4\text{-}15)$$

The output from the MUSTANG instrument is a sequence of 512 voltages. These voltages are directly proportional to the photon flux in 512 wavelength bands covered by the pixels. Expressed in decimal units per pixel, D, the instrument output may be written as;

$$D=RB_wP_\lambda \qquad (4\text{-}16)$$

where R is the instrument response in decimal units per photon per second per Å. B_w is the bandwidth in Angstroms. The instrument response (R) is the product of the various efficiencies and transfer functions of the individual components of the instrument. Although an in-depth study of the development of the instrument response would be beyond the scope of this thesis, a cursory treatment is germane to an overall understanding of how the MUSTANG operates. The following definitions will be used in this discussion:

- E_1 - efficiency (photon/photon) of the telescope mirror;
- E_2 - efficiency (photon/photon) of the Ebert mirror;
- E_3 - efficiency (photon/photon) of the diffraction grating;
- E_4 - quantum efficiency (el/ph) of the photo-cathode;
- G_{mcp} - gain (el/el) of the microchannel plates;
- E_5 - efficiency (ph/el) of the phosphor screen;
- E_6 - quantum efficiency (el/ph) of the photodiode;
- τ - integration period (sec);
- g_1 - transfer function (v/el) of the image detector amplifier;
- g_2 - transfer function (decimal units/v) of the analog to digital conversion.

Over one integration period, the output from a photodiode will be;

$$W_{pd}=P_{\lambda}(E_1E_2E_3G_{mcp}E_4E_5\tau) \tag{4-17}$$

in electrons per Angstroms. During this same time period, the instrument output will be;

$$D=W_{pd}(g_1g_2)B_w \tag{4-18}$$

decimal units per pixel. Substituting Equation (4-17) into the expression for the instrument output (4-18) and separating out the incoming flux results in;

$$D=P_{\lambda}(E_1E_2E_3G_{mcp}E_4E_5g_1g_2\tau)B_w. \tag{4-19}$$

Therefore the overall MUSTANG response, R, can be defined as;

$$R=(E_1E_2E_3G_{mcp}E_4E_5g_1g_2\tau). \tag{4-20}$$

Substituting the expression for flux (4-15) into equation (4-19) results in;

$$D=RB_w\left(\frac{A_tA_s}{\pi f^2}\right)\rho E_{\lambda}. \tag{4-21}$$

The constants above are gathered to define a new constant;

$$K=RB_w\left(\frac{A_tA_s}{\pi f^2}\right)\rho. \tag{4-22}$$

The output of the instrument can now be expressed as;

$$D=KE_{\lambda}. \tag{4-23}$$

The column emission rate for isotropic emissions is;

$$4\pi I = \int E(Z)\, dZ. \tag{4-24}$$

Where the limits of integration are from Z_0 to ∞, $4\pi I$ is the column emission rate and E is the omnidirectional volume emission rate at an altitude Z. Since the atmospheric emissions are omnidirectional the spectral radiance sensed by the MUSTANG is;

$$L_\lambda = \left(\frac{10^6 4\pi I}{4\pi}\right) \tag{4-25}$$

where $4\pi I$ is the intensity in Rayleigh/Å. Therefore, the output of the instrument due to the spectral radiance received from the atmosphere is;

$$D = RB_w \left(\frac{A_t A_s}{f^2}\right) L_\lambda. \tag{4-26}$$

Substituting the expression for spectral radiance (4-25) we obtain;

$$D = RB_w \left(\frac{A_t A_s}{f^2}\right) \left(\frac{10^6 4\pi I}{4\pi}\right). \tag{4-27}$$

We can now solve for the emission rate of the atmosphere;

$$4\pi I = \left(\frac{1}{10^6}\right) \left(\frac{4\pi f^2}{B_w R A_t A_s}\right) D. \tag{4-28}$$

The atmospheric emission rate ($4\pi I$) is in units of R/Å.

We now define a new constant;

$$C=\left(\frac{4\pi f^2}{10^6 B_v R A_t A_s}\right). \qquad (4\text{-}29)$$

Now using the expression (4-22) for the constant K derived from the laboratory calibration we obtain;

$$C=\left(\frac{4\rho}{10^6 K}\right). \qquad (4\text{-}30)$$

The constant C is the overall calibration parameter for the MUSTANG. K is determined from the laboratory constants equation (4-22) and the reflectance (ρ) is determined experimentally.The spectral emission rate from the atmosphere is equal to the calibration parameter times the detector response.

$$I=CD. \qquad (4\text{-}31)$$

The spectral calibration parameter, is depicted in Figure 9. Below 2000 Å molecular oxygen has absorption bands, so the calibration parameter is not accurate in this region. The MUSTANG has previously been calibrated in a vacuum to permit a sensitivity calibration below 2000 Å.(MACK 1990).

d. Calibrated Light Sources

In order to determine the laboratory constant K we must simulate the irradiance the MUSTANG senses in space. This was accomplished by using calibrated light sources. The lamps used for the calibration had been provided by the manufacturer with values of irradiance in dimensions of energy (Uw/cm^2 nm).

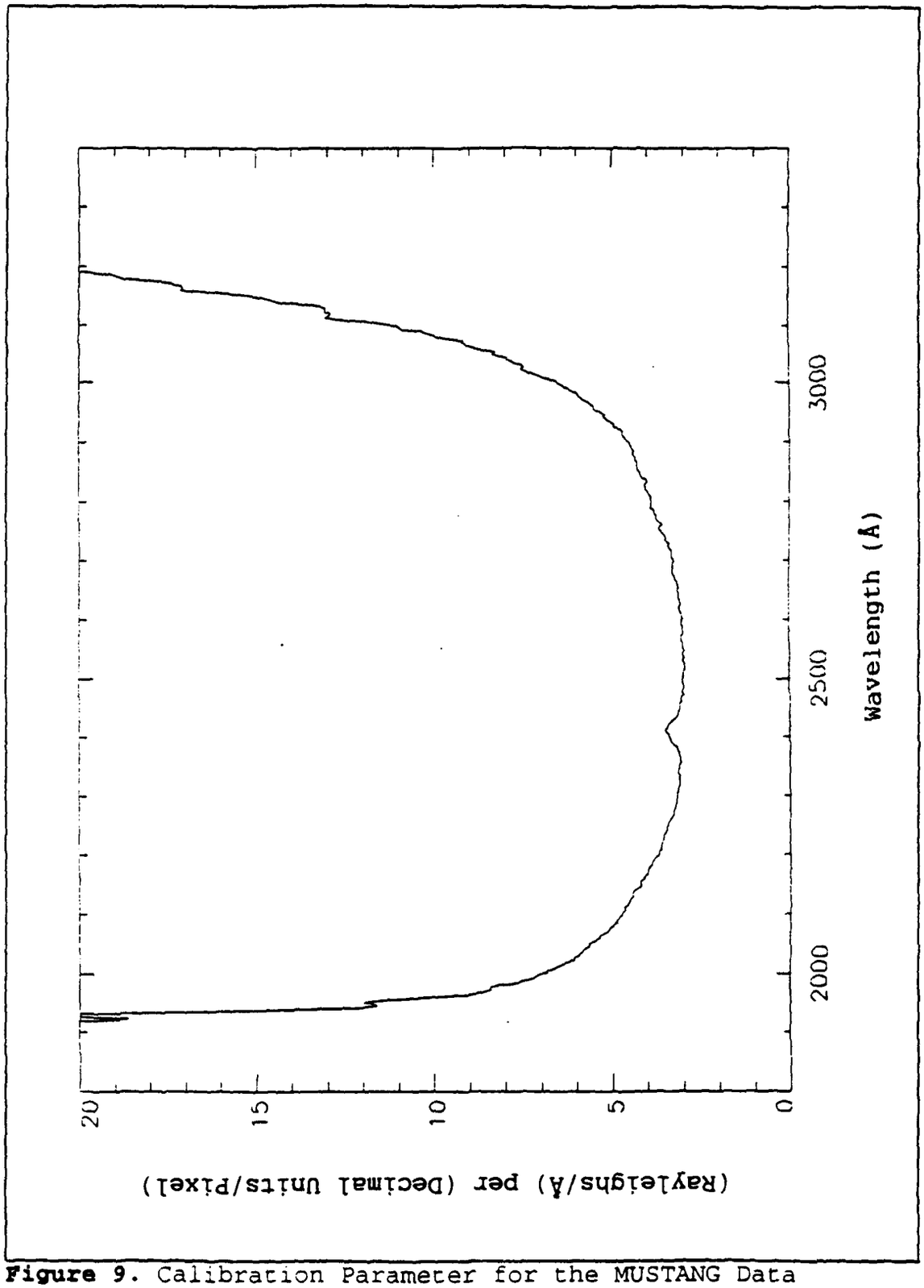

Figure 9. Calibration Parameter for the MUSTANG Data

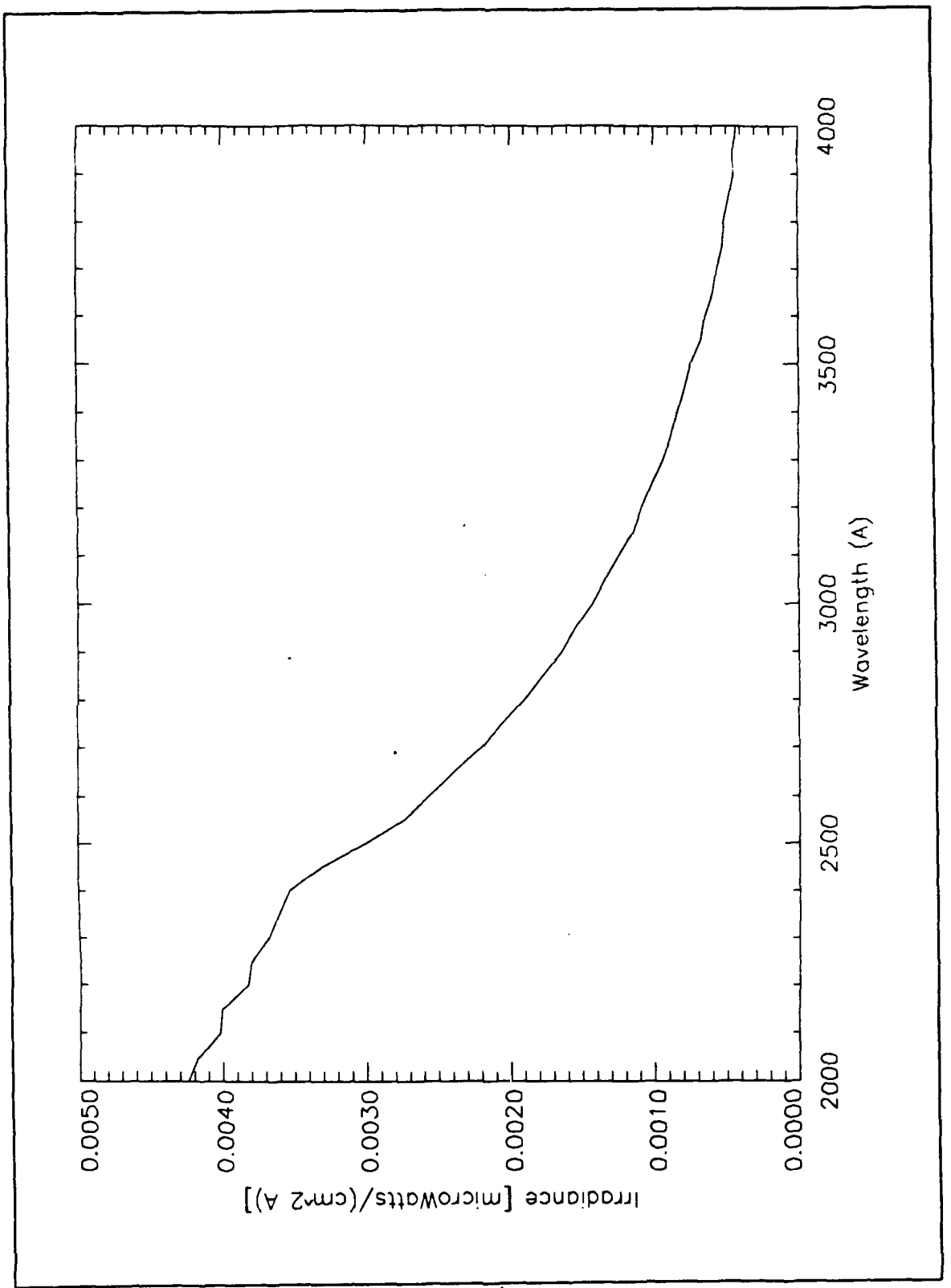

Figure 10. Irradiance of Deuterium Lamp

Table II. IRRADIANCE FROM FEL SOURCE AT 50 cm

WAVELENGTH (Å)	IRRADIANCE (uW/cm^2 nm)	IRRADIANCE (photons/cm^2 s Å)
2500	0.0179	2.2466E10
2600	0.0315	4.1116E10
2700	0.0522	7.0756E10
2800	0.0817	1.1484E11
2900	0.123	1.7907E11
3000	0.178	2.6808E11
3100	0.250	3.8907E11
3200	0.343	5.5103E11
3300	0.458	7.5877E11
3400	0.599	1.0224E12
3500	0.769	1.3512E12

The output of the MUSTANG is determined by the number of photons which strike the photodiode over one integration period. Therefore it was necessary to convert the manufacturers data into ph/cm^2 s Å. The manufacturers data for deuterium and FEL sources are depicted in Tables II and III.

To calibrate the MUSTANG instrument we must know the irradiance for each wavelength bin of the detector. For the Deuterium lamp, the manufacturers values were converted using the IDL linear interpolation algorithm called Interpol. For the FEL, a black body distribution was fit to the manufacturers data. The manufacturers curves are depicted in Figures 10 and 11.

e. Screen Reflectivity

The atmosphere, as observed by the MUSTANG instrument, is an extended and diffuse source. To simulate these conditions, the instrument was calibrated using a

Table III. IRRADIANCE FROM DEUTERIUM SOURCE AT 50 CM

Wavelength(Å)	Irradiance (uW/cm^2 nm)	Irradiance (photons/cm^2 s Å)
2000	4.246E-02	4.272E10
2050	4.180E-02	4.310E10
2100	4.027E-02	4.254E10
2150	4.011E-02	4.338E10
2200	3.830E-02	4.238E10
2250	3.807E-02	4.309E10
2300	3.690E-02	4.269E10
2350	3.620E-02	4.279E10
2400	3.542E-02	4.276E10
2450	3.315E-02	4.085E10
2500	3.006E-02	3.780E10
2550	2.744E-02	3.520E10
2600	2.566E-02	3.356E10
2650	2.385E-02	3.179E10
2700	2.202E-02	2.991E10
2750	2.058E-02	2.847E10
2800	1.908E-02	2.688E10
2850	1.782E-02	2.555E10
2900	1.647E-02	2.403E10
2950	1.553E-02	2.305E10
3000	1.431E-02	2.160E10
3050	1.344E-02	2.062E10
3100	1.253E-02	1.954E10
3150	1.152E-02	1.825E10
3200	1.087E-02	1.750E10
3250	1.015E-02	1.660E10
3300	9.426E-03	1.565E10
3350	8.850E-03	1.491E10
3400	8.457E-03	1.447E10
3450	7.920E-03	1.374E10
3500	7.499E-03	1.320E10
3550	6.824E-03	1.219E10
3600	6.467E-03	1.171E10
3650	5.994E-03	1.101E10
3700	5.664E-03	1.054E10
3750	5.233E-03	9.871E09
3800	5.216E-03	9.970E09
3850	4.802E-03	9.300E09
3900	4.499E-03	8.826E09
3950	4.486E-03	8.913E09
4000	4.381E-03	8.815E09

diffusing screen. The screen used for this purpose was a one foot square by one-quarter inch thick sheet of aluminum,

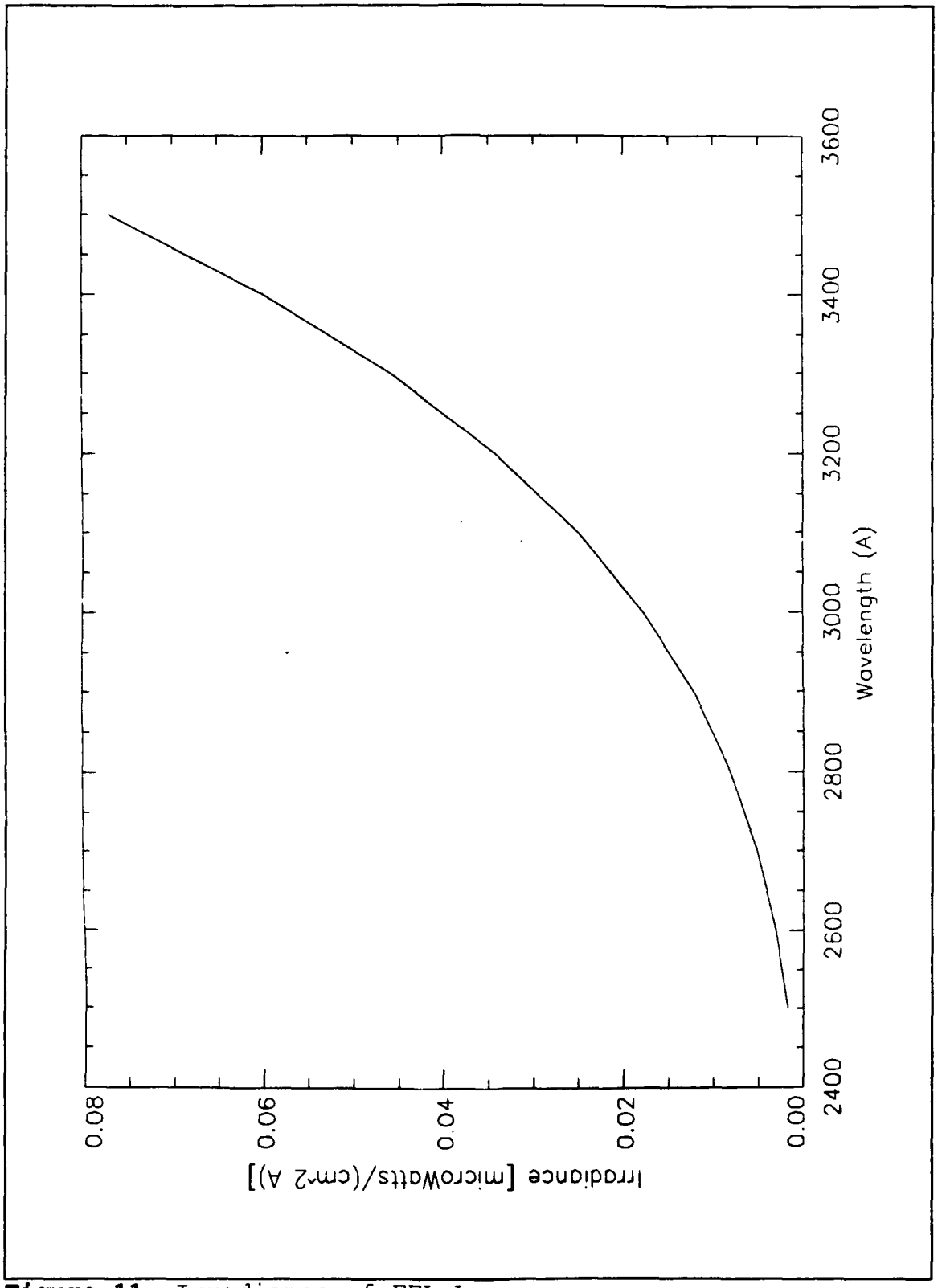

Figure 11. Irradiance of FEL Lamp

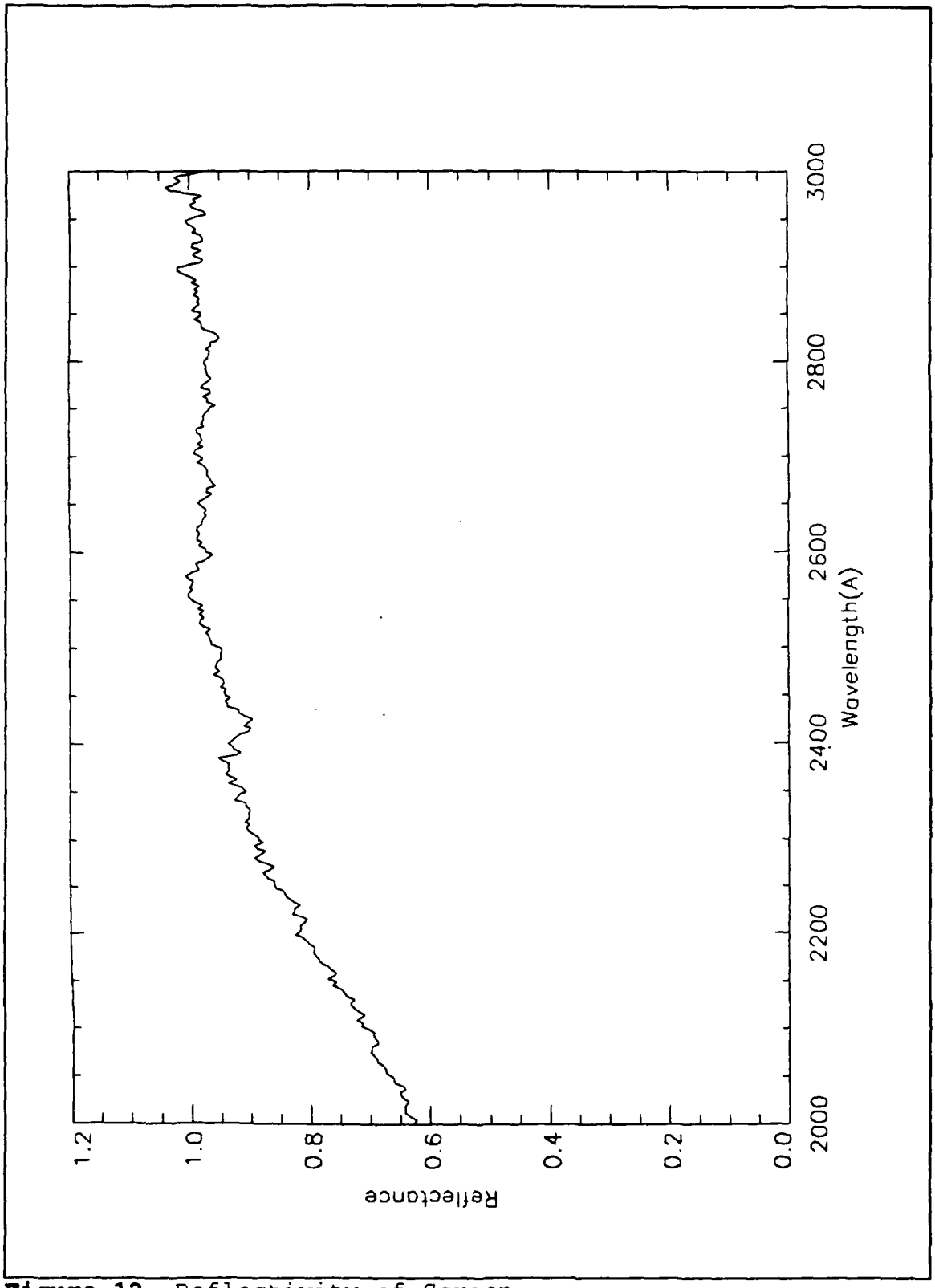

Figure 12. Reflectivity of Screen

coated with Barium Sulfate ($BaSO_4$) which has been proved to be stable when exposed to ultraviolet flux and environmental conditions, (Grum and Luckey 1968). The coating was applied using a high viscosity KODAK Model 13270 Laboratory Sprayer. Ten coats were applied to ensure optimal reflectance.

The reflectivity of the screen as a function of wavelength was determined by comparing the deuterium spectrum obtained using the diffusing screen to the spectrum obtained when the MUSTANG viewed the source directly through a pin hole. The ratio of the reflected to the direct measurements was then normalized. This procedure yielded a continuous curve of reflectance as a function of wavelength.

The direct measurements proved to be somewhat difficult. The detector would saturate when viewing the lamp directly. In order to correct this, the iris diaphragm was closed, a piece of black electricians tape was placed over the opening, and a pinhole was created in the tape. The irradiance was still sufficient to saturate the screen. Fortunately the elasticity of the tape caused the pinhole to shrink and, before completely closing, the irradiance was reduced sufficiently to prevent saturation of the detector, and so enable a measurement to be made.

The reflectance curve was normalized to the absolute reflectance of $BaSO_4$ at 2500 Å reported by Grum and Luckey . The IDL function poly_fit was used to fit the curve which produced a continuous function of reflectance with

wavelength. Figure 12 displays the reflectivity curve obtained from the screen. The reflectance of the curve was found to be approximately five percent lower than the values presented for the reflectance of barium sulfate (Grum and Luckey ,1968). The reason for the lower reflection was probably due to the method of application. The article by Grum and Luckey reports that spraying will not permit a sufficient thickness of $BaSO_4$ to be produced to achieve reflective values obtained with a 1.0 mm coating.

Table IV. MUSTANG INSTRUMENT RESPONSE AT 2318Å TO VARIOUS VALUES OF IRRADIANCE

vData Point	Relative Intensity	Distance (cm) Source to Screen	Distance Ratio
1	991	105.2	3.61
2	979	110.2	3.30
3	938	115.2	3.01
4	860	120.2	2.77
5	722	130.2	2.36
6	627	140.2	2.04
7	546	150.2	1.77
8	481	160.2	1.56
9	426	170.2	1.38
10	380	180.2	1.23
11	340	190.2	1.11
12	310	200.2	1.00
13	284	210.2	0.91
14	256	220.2	0.83
15	233	230.2	0.76
16	214	240.2	0.69
17	196	250.2	0.64
18	167	270.2	0.55
19	146	290.2	0.48
20	137	300.2	0.44

f. Linearity of Instrument Response

While in flight the detector is continuously taking spectra of atmospheric airglow from an altitude of 100km to 320km. Because of this altitude difference there is a great range in intensities of the airglow being recorded. We needed to determine how the MUSTANG instrument responded to a wide range of intensities. In other words we needed to determine the linearity of the instrument response.

This was accomplished by varying the distance of the deuterium lamp to the screen. The largest relative intensity occurred at pixel 150 or wavelength 2318 Å. The irradiance at the screen is proportional to the inverse of the square of the distance of the lamp to screen. This distance was changed in 10 cm increments and the intensity recorded at pixel 150. Since the other calibrations had been performed at 200 cm, we used this as our standard. The square of the ratio of 200 cm to other distances used in the experiment is referred to as the distance ratio. The results of the measurements are given in Table IV. A plot of the relative intensity versus the distance ratio is shown in Figure 13. The plot shows the instrument response is linear to an intensity of about 900 decimal units.

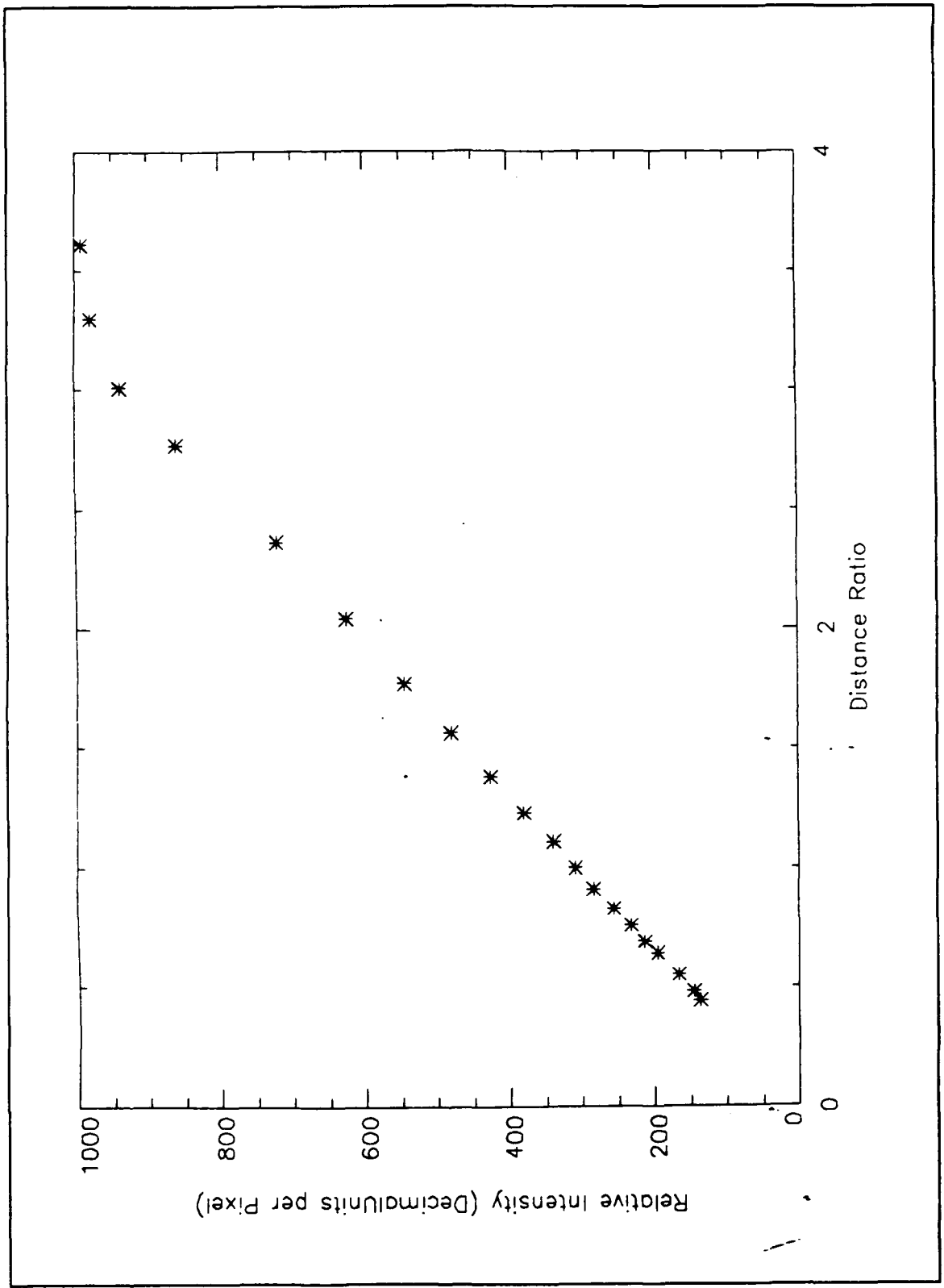

Figure 13. Linearity of MUSTANG Instrument Response

V. CONCLUSION

A. INTRODUCTION

The MUSTANG instrument was calibrated using standard techniques to determine the wavelength calibration, overall sensitivity and linearity of response. A calibration was performed prior to the March 19, 1992 rocket flight. A post-flight calibration revealed that there was no significant change (less than 2%) in instrument sensitivity as a result of the flight.

B. SUMMARY OF FINDINGS

Although the overall sensitivity did not change during the flight, the wavelength scale shifted approximately one pixel. We concluded that this probably occurred during the launch. The vibrations could have caused the diffraction grating to rotate slightly.

During the calibration we noticed about a twenty percent difference between the scaled intensities of the deuterium and FEL lamps. Further investigation revealed that the FEL lamp was the source of the problem. The FEL manufacturers manual states that a one percent difference in the current supplied to the lamp can result in a twelve percent intensity difference at 2500 Å. The FEL lamp was overdue for a

calibration and there was no record of the last calibration of the power supply.

C. RECOMMENDATIONS FOR FURTHER RESEARCH

An experiment to determine the instrument response as a function of time and temperature should be conducted in the laboratory. It has been suggested (Anderson, 1990) that a thermocouple on the driver/amplifier card of the detector would allow the monitoring of temperature and instrument response as a function of time. This would lead to a better understanding of the dynamics of the time/temperature relationship.

There exists a need for an aggressive calibration program for the lamps and power supplies. The calibration of these devices should be up-dated on a regular basis.

LIST OF REFERENCES

1. Anderson, Carl K., *A Calibration of the Naval Postgraduate School Middle Ultraviolet Spectrograph and an Analysis of the OII 2470 Å Emissions Obtained from Mid-Latitude Rocket Observations*, Master's Thesis, Naval Postgraduate School, Monterey, California, September, 1990.

2. Chapman, S., "The Absorption and Dissociation or Ionizing Effect of Monochromatic Radiation in the Atmosphere on a Rotating Earth", *Proc.Phy.Soc.43*, 26-45 and 483-501, 1931.

3. Grum, F., and Luckey, G.W., "Optical Sphere Paint and a Working Standard of Reflectance", *Applied Optics*, Vol.7, No.11, 1968.

4. Mack, Bryan D., *An Analysis of Middle Ultraviolet Emissions of Molecular Nitrogen and Nitric Oxide and Vacuum Calibration of an Ultraviolet Spectrograph*, Master's Thesis, Naval Postgraduate School, Monterey, California, June, 1991.

INITIAL DISTRIBUTION LIST

1.	Defense Technical Information Center Cameron Station Alexandria, Virginia 22304-6145	2
2.	Library, Code 0142 Naval Postgraduate School Monterey, California 93943-5002	2
3.	Dr. D.D. Cleary Physics Department, PH-CL Naval Postgraduate School Monterey, California 93943-5002	3
4.	Dr. S. Gnanalingam Physics Department, Ph-GM Naval Postgraduate School Monterey, California 93943-5002	1
5.	Lt. Bruce E. Chase 669 Creighton Road Orange Park, Florida 32073	2